LA-UR-80-108

TITLE: SHORT-PULSE CO_2-LASER DAMAGE STUDIES OF NaCl and KCl WINDOWS

AUTHOR(S): Brian E. Newnam
Andrew V. Nowak
Dennis H. Gill

SUBMITTED TO: Proceedings of 11th Annual Symposium on Optical Materials for High Power Lasers

MASTER

University of California

LOS ALAMOS SCIENTIFIC LABORATORY
Post Office Box 1663 Los Alamos, New Mexico 87545
An Affirmative Action/Equal Opportunity Employer

Form No. 836 R3
St. No. 2629

SHORT-PULSE CO_2-LASER DAMAGE STUDIES OF NaCl AND KCl WINDOWS

Brian E. Newnam, Andrew V. Nowak, and Dennis R. Gill
Los Alamos Scientific Laboratory
Los Alamos, New Mexico 87545

The damage resistance of bare surfaces and the bulk interior of NaCl and KCl windows was measured with a short-pulse CO_2 laser at 10.6 μm. Parametric studies with 1.7-ns pulses indicated that adsorbed water was probably the limiting agent on surface thresholds in agreement with previous studies at long pulsewidths. Rear-surface thresholds up to 7 J/cm^2 were measured for polished NaCl windows, whereas KCl surfaces damaged at approximately 60% of this level. The breakdown electric-field thresholds of exit surfaces were only 50% of the value of the bulk materials. The pulsewidth dependence of surface damage from 1 to 65 ns, in terms of incident laser fluence, increased as $t^{1/3}$.

Key words: Alkali halides; CO_2 laser; KCl; laser damage; laser fusion; NaCl; nanosecond pulse; surface damage.

1. Introduction

Large diameter NaCl windows are used extensively in the CO_2 amplifiers and target chambers of the Helios (10 kJ) and Antares (100 kJ, projected) fusion lasers at Los Alamos Scientific Laboratory (LASL). Since these large windows (46-cm diameter, 8.5-cm thick) represent a sizeable portion of the cost of building and maintaining these lasers, it is imperative that they have maximum optical damage resistance. In the experimental studies to be reported herein, we have examined some of the material and laser parameters that affect the surface and bulk damage of NaCl (and KCl) for short (≤1 ns) pulses at 10.6 μm.

At the 1978 Laser Damage Symposium, Kovalev and Lazzullov [1][1] presented substantial experimental evidence that adsorbed H_2O is the limiting agent on the front-surface (1-ns) damage thresholds of NaCl windows. They supported the hypothesis that this surface layer of water strongly absorbs the CO_2 radiation (10^4 cm^{-1} at 10.6 μm [2]), producing a rapidly expanding vapor front which, when a sufficiently low density is reached, allows electric field breakdown as described by the familiar Paschen curve. Their experiments were carried out with TEA CO_2 laser pulses having a high leading peak of 100-200 ns duration (≤150 ns risetime) and a long tail (1-15 μs) containing the majority of the pulse energy. Also, their studies were on the entrance surface. Since pulsewidths of interest to laser fusion are much shorter, ≤1 ns, we conducted a series of short pulse experiments on exit surfaces (the most susceptible to early failure) to determine if adsorbed water is also the primary agent of surface damage for these conditions. These are described in section 4.

Since surface damage precedes bulk damage in NaCl windows, we have also made a careful comparison of the bulk and surface thresholds of crystals from four prominent manufacturers to quantify the difference and learn how much potential improvement may be possible over presently used polishing methods. These results and a discussion are given in section 6.

As early as 1974, Stark and Reichelt [3] compared the damage resistance of Harshaw Polytran KCl and NaCl window surfaces using 1 ns pulses. They measured a fluence ratio of 0.5 in favor of NaCl. In the past five years, however, significant advances in the technology of crystal growth and surface polishing processes have occurred which suggested a new and more extensive comparison of KCl and NaCl thresholds. These results appear in section 7.

[1] Figures in brackets indicate the literature references at the end of this paper.

Finally, in section 8 we present our results for the pulsewidth dependence of exit-surface damage for NaCl and KCl windows.

2. Description of Test Specimens

Test specimens of NaCl and KCl were supplied by four prominent sources of high-quality ir crystals: Harshaw Chemical Company in Solon, Ohio (10 NaCl, 3 KCl), Naval Research Laboratory (NRL) in Washington, D.C. (1 NaCl, 1 KCl), Hughes Research Laboratories (HRL) in Malibu, California (1 NaCl, 1 KCl), and William Fredericks at Oregon State University (OSU) in Corvallis (2 NaCl). The details of these specimens are listed in table 1. To obtain a sufficiently long path length for conducting bulk-damage tests in the thin Harshaw windows, (without interference from concurrent front-surface damage) the perimeter of a few harshaw windows were also polished flat. Also, two of the Harshaw windows were later cleaved in air to allow a direct comparison of cleaved and polished surface thresholds.

Table 1. Description of NaCl and KCl test specimens

Supplier	Growth technique	Crystalline state	Surface state	Thickness
Harshaw	Stockbarger and Kyropoulos	single	polished with 0.3 μm Linde A	10 mm and 12 mm
HRL	Czochralski + CCl_4 KAF	single NaCl forged/polycrystal-KCl	polished 0.3 μm Linde A IKI etch-KCl	KCl: 9 mm NaCl: 10 mm
NRL	Czochralski + CCl_4 KAF	single	polished 0.3 μm Linde A	KCl: 55 mm NaCl: 53 mm
OSU	ion exchange	single	cleaved	11 & 24 mm

3. Experimental Apparatus and Procedure

Laser pulses of 1.7 ns to 65 ns (FWHM) at 10.59 μm (P-20) were emitted from a gain switched CO_2 oscillator/double-pass amplifier in LASL's Gigawatt Test Facility. This laser provided a single-longitudinal mode, single line, and gaussian spatial profile output every 20 seconds which was ideal for these single-shot per site (1-on-1) tests. The short pulses were sliced out of the 65-ns oscillator emission by use of a double Pockel cell/spark gap arrangement. As illustrated in figure 1, the temporal shape of these short pulses was asymmetric (300 ps risetime, 1.5 ns falltime, 10-90% levels). A fairly large laser-beam spot size, 1-mm radius at the $1/e^2$ level, was used on the majority of the surface threshold tests. Samples were placed ahead of the focus of a 1-m f.l. plano convex lens for these tests. For use in comparison of bulk and surface thresholds, a spot-size radius of 0.14 mm was obtained at the focus of a 19 cm f.l. lens. The spatial profile, measured periodically by a pinhole scan, approximated a gaussian dependence. The energy, temporal and spatial diagnostics, indicated in figure 2, have been previously described [6], and a summary of the laser test parameters is given in table 2.

Table 2. CO_2 laser damage test parameters

Wavelength	P(20), 10.59 μm, single mode TEM_{00}
Pulsewidths	1 to 65 ns (FWHM)
Spot size radius	0.15 to 1.5 mm
1-on-1 irradiation	40 to 60 sites
Test environment	Air at 600 torr (2,200 meters alt.)

The criterion for surface damage was permanent disruption (pitting or increased light scatter) visible under bright, white light illumination with a 90X stereo microscope. Isolated microbubbles occurred at the threshold of bulk damage. Generally, microsparks preceded the occurrence of visible damage by a small margin.

Measurements of the exit-surface and bulk-thresholds were satisfactorily conducted in air rather than in the vacuum environment chosen by Faizullov and Kovalev [1] for most of their front-surface tests. Front-surface tests of high-threshold materials in air are often plagued by air breakdown at the pulse peak which effectively prevents energy in the tail of the pulse from reaching the surface. We determined that in measuring exit-surface thresholds, the interference of air sparks was not significant when viewing with the white light microscope method. Previously, Hayden and Liberman [5] had found the exit-surface thresholds of a NaCl window in vacuum and air to be essentially the same, 5.7 and 5.4 J/cm^2, respectively.

The transmitted temporal-pulse termination technique of detecting damage was not considered sufficiently sensitive in these tests with large millimeter-size beams. The area of the damage sites (microns in diameter) was judged much too small to block a significant fraction of the pulse energy.

Exit-surface rather than front-surface damage was of primary interest in these studies since, for low-index materials like NaCl, the former almost always occurs first. This derives from the in-phase addition of the incident and reflected electric vectors at the rear surface as indicated in figure 3. However, for normal incidence of a coherent laser beam upon a window having parallel surfaces, the ratio of the front-to-rear-surface thresholds (in MV/cm) is dependent on the thickness and can range from 1 to 4 [6]. Therefore, in these tests the windows were oriented sufficiently off normal (several degrees) to preclude multiple-beam interference effects.

4. Damage Morphology

Threshold damage on the exit surfaces was in the form of one or a few shallow microspits, of the order of several microns diameter. Invariably, a separate microspark was associated with each damage site, but sparks did occur at lower laser fluences with no discernible damage. On some surfaces, the pits were elliptically shaped with the long axes parallel to polish streaks.

Evidence of threshold damage in the bulk was in the form of one or a few tiny bubbles remaining after an incandescent microspark(s). High-magnification studies of these bulk sites were not completed upon this writing.

5. Influence of Adsorbed Water

In addition to schlieren photographs to establish the existence of an expanding vapor front at an irradiated NaCl surface, Kovalev and Faizullov [1] supported their assertion that adsorbed water determines the surface damage threshold with the following evidence:

1) As the laser spot size was varied over the range 0.12 to 1.12 mm radius, the 1-on-1 threshold of NaCl in vacuum was constant at 16 MV/cm^2 (2.2 J/cm^2). The tests were conducted at 10.6 μm with a 150 ns pulse risetime. This result was theoretically predicted by their eq. 5 for spot sizes larger than the thickness of an adsorbed water film uniformly absorbing over the surface.

2) The 1-on-1 threshold increased with pressure of the ambient gas. This was expected because the shock wave velocity of an expanding water vapor front is reduced at higher ambient pressures, and there is an increased frequency of electron-collisions with neutral particles. Thus, for full development of an electron avalanche in the rarefied region, a higher electric field is required.

3) After an initial dramatic rise in threshold from 2.2 to 11.5 J/cm^2 by treating an NaCl surface with an HCl acid etch, the threshold dropped, upon subsequent remeasurement at 30 minutes, to a value of 6.5 J/cm^2. This value appeared to be a steady-state level as determined from additional periodic measurements up to 1 month. Readsorption of ~ monolayer within 20 minutes was indicated.

4) Kovalev and Faizullov [1,7] observed large increases in the 1-on-1 threshold of NaCl when pre-irradiated at subthreshold fluences (N-on-1 effect). Removal of volatile absorbing contaminants, such as water, was indicated.

In view of these important results conducted with long pulses, the present study with 1.7-ns CO_2 pulses was motivated. To detect the possible influence of adsorbed H_2O on NaCl surface thresholds the following tests were conducted:

1. threshold versus spot size,
2. threshold of a cleaved surface versus time of ambient exposure, and
3. threshold versus total water content.

5.1. Threshold versus Spot Size

Figure 4 exhibits the exit-surface threshold measurements of one NaCl window for spot-size radii from 0.14 to 1.5 mm. The vertical bars for each point represent the threshold variation across the sample surface. Therefore, the solid line drawn through the points could as well have been drawn horizontally, i.e., no spot-size dependence was evident. Similar measurements on two other windows also revealed no definite dependence.

5.2. Threshold of a Cleaved Surface

The 1-ns threshold of an NaCl window cleaved in air (relative humidity of 15%) was determined within one hour to be 17.6 ± 0.6 J/cm^2. After ten days exposure, the threshold had dropped to 14.1 ± 1.5 J/cm^2, a decline of 20%.

These tests were performed on the front surface, instead of the rear surface as were all other of our tests, because rear-surface tests were not possible at these high-fluence levels. When the cleaved surface was oriented as the rear surface, the polished (front) surface damaged first, thereby shielding the rear surface of interest. Using the polished samples available, it was not possible to obtain satisfactory cleaved surfaces for both front and rear.

5.3. Threshold versus Total Water Content

The presence of OH^- ions in NaCl is revealed by the characteristic spectral absorption peak at 187 nm, near the uv band edge [8,9]. As seen in figure 5, there was a wide range of OH^- concentrations (bulk + surface) among the test specimens grown by the several techniques. OSI sample No. 1 65 was purposely grown with a slight water concentration. The 187-nm absorbance of the Harshaw sample, No. 1 48-14 greatly exceeded that of the other samples supplied by Harshaw. In table 2, we compare the absorbance with the exit surface threshold. It is appropriate to compare the results for the cleaved and polished windows separately. The cleaved window with greater OH^- concentration did have a lower threshold, but the polished Harshaw sample with very high absorbance actually had a slightly higher threshold than the HRL sample with low OH^- content.

Table 2. NaCl exit-surface threshold versus absorbance at 187 nm

Sample	Absorbance at 187 nm[a]	Exit threshold J/cm^2	Exit threshold GW/cm
OSI - ion exchange 4 65 cleaved	0.10	7.0	1.1[b]
HRL - KAlF$_4$ forged Polished	0.10	5.4	1.0[a]
OSI - ion exchange 1 65 cleaved	0.0[c]	5.4	1.0[b]
Harshaw - Stockbarger 1 48 14, heel, polished	1000	6.1	1.1[a]

[a] $\lambda = 1.0$ mm, $\Delta t = 1.7$ ns (FWHM)

[b] See table 1 for sample thicknesses.

5.4. Discussion

The absence of a spot-size dependence and the decline of the surface threshold with time for our 1.7-ns pulses are similar to the results obtained by Kovalev and Faizullov [1,7]. Correlation of the total OH^- ion content (bulk + surfaces) was not as conclusive, however. Direct correlation of the surface absorption at 187 nm with surface threshold would have been better. Unfortunately, surface absorption measurements of these relatively thin samples was not accomplished. However, the one clearly valid comparison of the surface thresholds of the two cleaved OSU crystals was consistent with absorption in a surface layer of water. Thus, the results of our three tests do support the hypothesis that surface damage of NaCl, for 1-ns CO_2 pulses, results from OH^- absorption.

Our observation that microsparks were associated with the tiny damage sites was not unexpected. At surface defects (scratches, pits or included polishing residue) the local electric field is enhanced, resulting in early breakdown most likely in the expanding vapor. The presence of the localized plasmas causes total retro-reflection and a maximum standing-wave field of 2.0 at the exit surface, as described by Boling et al. [10]. Early damage is a natural consequence.

Self-focusing, as a contributor to early breakdown of the exit surfaces, was also assessed. As reviewed in the Appendix, the magnitude of this effect in the above tests and those yet to be described was negligible.

6. Surface versus Bulk Thresholds

In table 4, the bulk and surface thresholds of NaCl crystals from four sources are compared. In computing the listed values, the enhancement of the electric field at the exit surface (recall figure 1) was taken into account. It is remarkable that the same value, 2.1 MV/cm, was obtained for the bulk threshold for each of the first three samples listed. The ratio of exit-surface to bulk thresholds for these was also about the same, ~ 5. In terms of incident laser fluence (J/cm^2), exit surfaces polished by standard methods survived approximately 20% as much as the bulk (25% for front surfaces).

Table 4. Comparison of bulk and exit-surface thresholds of NaCl single crystals

Sample	Bulk	Surface	Ratio
	MV/cm	MV/cm	
Harshaw 6-8-16 Stockbarger	2.1 ± 0.1	1.04	0.47
NKI RAP B 64	2.1 ± 0.1	1.15 ± 0.10	0.55
PRI RAP 78 179	2.1 ± 0.1	1.07 ± 0.04	0.51
OSU ion exchange 20 2.14, a 65	1.02 ± 0.01	1.20 ± 0.11 (cleaved, 10 years ago (1965))	1.17

w 0.14 mm
Δt 1.7 ns (1/e²)
λ 10.6 μm

The bulk threshold of the OSU crystal was much lower than anticipated, especially since its concentration of impurities was very low [11]. Tiny scattering sites were visible in the bulk by use of a He-Ne laser (forward scattering, mainly). As this crystal was grown in an atmosphere of argon, it has been suggested (unconfirmed as yet) that the scattering sites were bubbles of argon gas [11]. For a spherical void in NaCl (n = 1.49 at 10.6 μm) an electric field enhancement factor of 1.24 is predicted from Bloembergen's

analysis [12]. The remainder of the difference may be accounted for by breakdown in argon gas at some unknown pressure rather than in bulk NaCl. The threshold of this cleaved surface was unexpectedly high especially considering that the crystal was grown, cleaved and cleaned in 1965, 14 years ago!

There are several explanations why thresholds of surfaces are lower than in the bulk. Firstly, the E-field enhancement at the exit-surface results in earlier damage there than in either bulk or front surface. Secondly, the surface roughness produced by polishing results in enhanced electric fields and increased absorption. (At 1.06 μm, House et al. [13] found that fused silica surface-thresholds (MV/cm) were inversely proportional to the square root of the rms roughness.) Thirdly, polishing physically disrupts the crystalline order of a surface layer. Fourthly, polishing compounds and pitch are embedded and cleaning methods cannot be 100% effective. Fifthly, adsorbed gases, e.g., H_2O, absorb the laser energy. Absorption is augmented by surface roughness and embedded impurities.

To quantify the deleterious effect of polishing on the damage threshold, we tested two samples cleaved in air. The results, given in table 4, provide a comparison of 1-s thresholds of adjacent polished and cleaved surface areas. First, we note that the roughness of the cleaved surfaces (≈50 Å) was one-quarter that of the polished surfaces as measured with a profilometer. Therefore, it is not too surprising that the cleaved surfaces had much higher thresholds, by factors of 2.4 and 2.0, respectively in terms of laser fluence. The fact that these values were only 75 to 80% of the bulk electric-field thresholds (2.1 MV/cm) indicated that the finite roughness (50 Å) may have been a limiting factor. Sufficient moisture adsorbed during the one-hour test period may have also depressed the damage resistance. The reduced threshold after ten days exposure to ambient conditions was already discussed in section 5.2.

Table 4. Entrance surface thresholds of cleaved and polished NaCl (single-crystal).

Surface		Threshold J/cm²	Threshold MV/cm	Ratio of surface to bulk
Polished, ≈ 200 Å RMS				
Linde A - 0.3 μm	A	8.4 ± 1.0	1.09	0.52
1 year storage	B	9.0 ± 0.8	1.14	0.54
Cleaved, ≈ 50 Å RMS				
Tested within 1 hour in 35% RH	A	19.4 ± 2.4	1.66	0.79
	B	17.6 ± 0.6	1.58	0.75
After 10 days in 35-40% RH	B	11.1 ± 1.5	1.47	0.67

w 0.75 mm
Δt 1.7 ns (FWHM)

Sample A: Bicshaw E-24-20 (Kyropoulos)
Sample B: Bicshaw 6-1-16, Heel No. 1 (Stockbarger)

The 1-s thresholds given in table 4 may be compared with their exit-surface thresholds to obtain the ratio. For Sample A, these were 8.6/6.8 or 1.26 and for Sample B, these were 9.0/6.1 or 1.48. These compare well with the theoretical value of 1.56.

Addressing the problem of surface contamination by polishing compounds and pitch, we subjected two polished surfaces to Auger analysis. To our surprise, no evidence of Al was seen in the surface polished with Linde A (Al_2O_3), nor was carbon found in the surface polished with diamond paste! Examination with a more sensitive technique is suggested as the null result was unexpected. Previously, Turk et al. [14] had presented definite evidence of removal of an absorbing layer on a polished NaCl surface removable by use of an etchant (see figure 6). Presumably, the absorbing impurities were the Linde A, pitch and water.

We measured no difference in the surface thresholds of Harshaw Polytran NaCl (forged, polycrystalline) and Harshaw single-crystal material. However, no measurement of the bulk threshold of Polytran was made.

7. KCl versus NaCl

7.1. Bulk and Surface Measurements

The bulk thresholds of both NaCl and KCl, measured with relatively large beams (w = 0.14 mm radius) and 1.7-ns pulsewidth, are presented in table 5. Included for comparison are the data of Soileau et al. [15] and Fradin et al. [16] both of whom tested Harshaw crystals with very small spot-sizes and longer pulseforms. Although the value for NaCl is consistently the same, 2.1 MV/cm, the thresholds for KCl varied more widely. Since Harshaw has not concentrated on the growth of KCl windows for high-power, short-pulse use to the extent that they have for NaCl [17], we believe that the NRL sample of KCl better represents the presently attainable damage resistance for that material.

Table 5. Comparison of bulk thresholds of single crystal NaCl and KCl.

Source	Test Conditions	Bulk Thresholds, MV/cm NaCl	KCl	Ratio
NRL - RAP	a	2.1 ± 0.1	1.66 ± 0.09	0.79
Harshaw - Stockbarger	a	2.1 ± 0.2	0.76 ± 0.01	0.47
Harshaw - Stockbarger	b	2.1	1.45	0.69
	c	1.95	1.39	0.71

[a] At 1.7 ns (FWHM), w = 0.14 mm.

[b] At 60 - 105 ns (FWHM), partially mode-locked train, w = 0.036 mm; data of Soileau et al. [15].

[c] At 200 ns (FWHM), w = 25 μm, data of Fradin et al. [16].

As the exit-surfaces present the real limitation to high-power laser applications, we extended this comparison to polished surfaces of both crystals. The results, listed in table 6, continue to show NaCl as having the advantage. Using the mean values for the sets of samples measured, a fluence ratio of 0.61 was obtained. The corresponding field ratio is then 0.79, which is the same as that derived from the highest bulk values in table 5.

Table 6. Comparison of exit-surface thresholds of polished NaCl and KCl

Source	Single-crystal NaCl J/cm²	KCl J/cm²	Ratio
Harshaw	6.0 ± 0.5[a]	3.6 ± 0.6	0.60
NRL	6.2 ± 1.0	4.1 ± 0.8	0.66
NRL	5.1 ± 0.4	3.7 ± 0.4 (forged)	0.70
	KCl	4.8[b]	0.63
	NaCl	6.0[c]	

w = 1.0 mm, Δt = 1.7 ns (FWHM), λ = 10.6 μm, 1 on 1.

[a] Mean value of eight samples.

[b] Mean value of three samples.

[c] Mean value of ten samples.

7.2. Discussion

Based on arguments involving medium polarizability and available electrons (in pure, defect-free crystals) to contribute to an electron avalanche, one would expect that the damage threshold (MV/cm) would scale proportionately to atomic density divided by $n^2 - 1$. Such a derivation was obtained by Bettis et al. [18]. The values of (Atomic Density)/(n^2-1) for KCl and NaCl at 10.59 μm are 0.288 and 0.362. The ratio of these values is 0.80, which is the same as that obtained from the experimental measurements. Using the data generated by Fradin et al. [16], we constructed a plot of E_{th} (MV/cm) versus the above expression as seen in figure 7. An exact linear relationship is not expected since some of the physical properties of the crystals (impurities, defects, mechanical strength, melting point) are not included in the derivation of the abscissa. However, the general trend is obvious. Such a dependence has been observed for crystals and thin film materials at other wavelengths, e.g., by Bettis et al. [18] at 1.06 μm and by Newnam and Gill [19] at 266 nm.

Using their recent theory of electron avalanche breakdown, Sparks et al. [20] have computed bulk thresholds for KCl and NaCl at 10.6 μm to be 0.63 and 0.8 MV/cm, respectively. These computed values are obviously too low in light of experimental values presented here, but their ratio, 0.8, is in agreement with our measurements.

8. Pulsewidth Dependence

The exit-surface thresholds of several samples were measured with 65 ± 3-ns pulses as well as the short, 1.7-ns pulsewidth used as the standard in this test program. The smooth temporal structure of both pulseforms is seen in figure 1. Due to a difference in the beam divergence of the laser in the long-pulse mode, a larger spot-size radius (1.4 mm) was inadvertantly used. However, as demonstrated earlier in figure 4, the thresholds were not spot-size dependent, so a direct comparison with the 1.7-ns results (1.0-mm spot size) was deemed appropriate. The results for three samples are plotted in figure 8. Consistently, a straight line drawn between the data points exhibited a $t^{1/3}$ fluence dependence. For a few other samples, not plotted here, a slightly less-rapid increase with pulsewidth was measured. Since tiny microsparks were generally associated with damage at isolated surface sites, it is not understood why the anticipated $t^{1/2}$ dependence (generally associated with diffusion processes such as plasmas) was not observed. Possible explanations include the rate of vapor expansion or the susceptibility of surface defects.

9. Summary

This study of the extrinsic surface and bulk thresholds of NaCl and KCl windows with millimeter-diameter, 1.7-ns CO_2 laser pulses at 10.59 μm has yielded some very significant results.

First, exit-surface damage, which occurs at 70% the fluence level of entrance-surface damage, was examined. Thresholds up to 7 J/cm^2 were measured for polished surfaces. In contrast, cleaved surfaces with one-quarter as much surface roughness damaged at twice the level of polished surfaces, but remeasurement after ten days found the advantage to have dropped to 50%. No spot-size dependence was observed for beam diameters from 0.4 to 3 mm. Correlation of the damage susceptibility with the total absorption (bulk + surfaces) at the OH$^-$ ion absorption band at 187 nm was not totally conclusive. Overall, however, the results of these experiments support the hypothesis [1,7] that surface damage results from OH$^-$ absorption, coupled with surface roughness.

That there is much room for improvement of the damage resistance of both NaCl and KCl surfaces was determined from comparative measurements of the bulk thresholds. Exit surfaces, with present state-of-the-art polish, damaged at only 50% of the electric-field threshold of the bulk, or at only a 20% level in terms of incident laser fluence (J/cm^2). For ideal surfaces, the thresholds at the exit could be as high as 70% as the bulk level (J/cm^2). Further work on surface preparation should be the first priority.

A comparison of the bulk and surface thresholds of KCl and NaCl produced by three vendors obtained a field ratio (MV/cm) of 80% in favor of NaCl. This is in agreement with theoretical predictions based on the electron-avalanche mechanism. Finally, a pulsewidth

dependence of $t^{1/3}$ was measured for a few samples of both materials from 1.7 to 65 ns, which was less than the anticipated $t^{1/2}$ dependence.

10. Acknowledgments

The authors are grateful for the cooperation of the following men for supplying the test specimens: David Krus and Ontario Nestor of Harshaw, Roger Turk and James Harrington of HRL, William Fredericks of OSU and Philipp Klein of NRL. Additionally, one of the authors (BN) is indebted to the above and Guy Bastien and Virgil Straughan of Harshaw for thorough discussions about crystal-growth technology, window shaping and surface polishing. Thanks go to Vito Lazazzera and Linda Martinez of LASL for polishing assistance and Robert Springer for Auger surface analysis. Leon Sonntag and John Meier provided invaluable assistance in carrying out the damage tests.

References

[1] Kovalev, V. I., and Faizullov, F.S., "Investigation of the Surface Breakdown Mechanism in IR-Optical Materials," in Laser Induced Damage in Optical Materials: 1978, (A. J. Glass and A. H. Guenther, eds.), p. 318. NBS Spec. Pub. 541, U.S. Gov't. Printing Off., Washington, D.C., (1978).

[2] Hale, G. M., and Querry, M. R., "Optical Constants of Water in the 200-nm to 200-μm Wavelength Region," Appl. Opt. 12, 555 (1973).

[3] Stark, E. E., Jr., and Reichelt, W. H., "Damage Thresholds in ZnSe, A/R Coated NaCl and Micromachined Mirrors by 10.6 μm Multijoule, Nanosecond Pulses," in Laser Induced Damage in Optical Materials: 1974, (A. J. Glass and A. H. Guenther, eds.), p. 54. NBS Spec. Pub. 414, U. S. Gov't Printing Off., Washington, D.C., (1974).

[4] Newnam, B. E. and Gill, D. H. "Damage Resistance of AR-Coated Germanium Surfaces for Nanosecond CO_2 Laser Pulses," in Laser Induced Damage in Optical Materials: 1977, (A. J. Glass and A. H. Guenther, eds.), p. 298. NBS Spec. Pub. 509, U.S. Gov't Printing Off., Washington, D.C. (1978).

[5] Hayden, J. J. and Liberman, I., "Measurements at 10.6 μm of Damage Threshold in Germanium, Copper, Sodium Chloride, and Other Optical Materials at Levels up to 10^{10} W/cm^2," in Laser Induced Damage in Optical Materials: 1976, (A. J. Glass and A. H. Guenther, eds.), p. 171. NBS Spec. Pub. 462, U.S. Gov't Printing Off., Washington, D.C., (1976).

[6] Sam, C. L., "Laser Damage of GaAs and ZnTe at 1.06 μm," Appl. Opt. 12, 878 (1973).

[7] Kovalev, V. I., and Faizullov, F. S., "Influence of Adsorbed Water on the Optical Strength of Infrared Optics Elements," Sov. J. Quantum Electron. 7, 326 (1977).

[8] Etzel, H. W. and Patterson, D. A., "Optical Properties of Alkali Halides Containing Hydroxyl Ions," Phys. Rev. 112, 1112 (1958).

[9] Rolfe, J., "Hydroxide Absorption Band in Alkali Halide Crystals," Phys. Rev. Lett. 1, 56 (1958).

[10] Boling, N. L. Crisp, M. D., and Dube, G., "Laser Induced Surface Damage," Appl. Opt. 12, 650 (1973).

[11] Fredericks, W. J., Oregon State University, personal communication, 1979.

[12] Bloembergen, N., "Role of Cracks, Pores, and Absorbing Inclusions on Laser Induced Damage Threshold at Surfaces of Transparent Dielectrics," Appl. Opt. 12, 661 (1973).

[13] House, R. A., II, Bettis, J. R., and Guenther, A. H., "Surface Roughness and Laser Damage Threshold," IEEE J. Quantum Electron. QE-11, 861 (1977).

[14] Turk, R. R., Pastor, R. C., Timper, A. J., Braunstein, M., and Heussner, G. K., "Optical Finishing of KCl Windows to Minimize Absorption in the Infrared," in Proc. of the Fifth Conf. on High Power Infrared Laser Window Materials-1975, (C. R. Andrews and C. L. Strecker, eds.), p. 103, DARPA, (1976).

[15] Soileau, M. J., Bass, M., and Van Stryland, E. W., "Frequency Dependence of Breakdown Fields in Single-Crystal NaCl and KCl," in Laser Induced Damage in Optical Materials: 1978, op. cit., p. 309.

[16] Fradin, D. W., Yaklonevitch, E., and Bass, M., "Comparison of Laser Induced Bulk Damage in Alkali-Halides at 10.6, 1.06, and 0.69 Microns," in Laser Induced Damage in Optical Materials: 1972, (A. J. Glass and A. H. Guenther, eds.), p. 27. NBS Spec. Pub. 372, U. S. Gov't Printing Off., Washington, D.C., (1972); also Appl. Opt. 12, 700 (1973).

[17] Krus, D. J., Harshaw Chemical Co., private communication, 1979.

[18] Bettis, J. R., House, R. A., Guenther, A. H., and Austin, R., "The Importance of Refractive Index, Number Density, and Surface Roughness in the Laser-Induced Damage of Thin Films and Bare Surfaces," in Laser Induced Damage in Optical Materials: 1975, (A. J. Glass and A. H. Guenther, eds.), p. 289. NBS Spec. Pub. 435, U. S. Gov't Printing Off., Washington, D.C., (1976).

[19] Newnam, B. E., and Gill, D. H., "Ultraviolet Damage Resistance of Laser Coatings," in Laser Induced Damage in Optical Materials: 1978, op. cit., p. 190.

[20] Sparks, M., Holstein, T., Warren, R., Mills, D. L., Maradudin, A. A., Sham, L. J., Loh, E., Jr., and King, F., "Theory of Electron-Avalanche Breakdown in Solids," in Laser Induced Damage in Optical Materials: 1979, (H. E. Bennett, A. J. Glass, A. H. Guenther, and B. E. Newnam, eds.), NBS Spec. Pub. 586, U. S. Gov't Printing Off., Washington, D.C., (1980).

[21] Wang, C. C., and Baardsen, E. L., "Study of Optical Third-Harmonic Generation in Reflection," Phys. Rev. 185, 1079 (1969), and Phys. Rev. B1, 2827 (1970).

[22] Maker, P. D., and Terhune, R. W., "Study of Optical Effects Due to an Induced Polarization Third Order in the Electric Field Strength," Phys. Rev. 137, A801 (1965).

[23] Smith, W. L., Bechtel, J. H., and Bloembergen, N., "Picosecond Breakdown Studies: Threshold and Nonlinear Refractive Index Measurements and Damage Morphology," in Laser Induced Damage in Optical Materials: 1975, op. cit., p. 321.

[24] Watkins, D. E., Phipps, Jr., C. R., and Thomas, S. J., "Ellipse Rotation in Germanium," in Digest of Technical Papers, 1979 IEEE/OSA Conf. on Laser Eng. and Applications, p. 31 (1979).

[25] Akhmanov, S. A., Sukhorukov, A. P., and Khokhlov, R. V., "Self-Focusing and Diffraction of Light in a Nonlinear Medium," Sov. Phys.-Usp. 10, 609 (1968).

[26] Kerr, E. L., "Transient and Steady-State Electrostrictive Laser Beam Trapping," IEEE J. Quantum Electron. QE-6, 616 (1970).

[27] Dawes, E. L., and Marburger, J. H., "Computer Studies in Self-Focusing," Phys. Rev. 179, 862 (1969).

[28] Marburger, J. H., "Self-Focusing Theory," Prog. Quant. Electr. 4, 35 (1975).

[29] Fradin, D. W., "The Measurement of Self-Focusing Parameters Using Intrinsic Optical Damage," IEEE J. Quantum Electron. QE-9, 954 (1973).

Appendix

Measurement of the extrinsic damage thresholds of NaCl and KCl with large laser beams ($w = 0.14$ mm for the bulk; 0.14 to 1.5 mm for surfaces) required substantial input powers. At these power levels, intensification of the laser radiation by self-focusing had to be carefully evaluated. Our analysis of the magnitude of self-focusing in the present tests included contributions from both fast (electronic) and transient (electrostrictive) nonlinear mechanisms. For the laser parameters and sample dimensions used, the computed nonlinear intensification was of negligible magnitude as we now review.

For a gaussian beam, the critical power for maintaining a constant shape is given by the familiar expression

$$P_1 = c\lambda_o^2 / 32\pi^2 n_2 \quad , \tag{1}$$

where $n = n_o + n_2\tilde{E}^2$, and where n_2 is a composite of nonlinear indices including n_{2e} and n_{2s}, representing the relatively prompt electronic and time-dependent electrostrictive material responses. For NaCl and KCl the values of n_{2e} used here were 4.6 and 3.7 x 10^{-13} esu, respectively. These values are the average of three sets of measurements in the visible and at 1.06 μm [21,22,23]. In a recent measurement at 10.6 μm of ellipse rotation in NaCl, Watkins et al. [24] also determined that n_{2e} was less than 6 x 10^{-13} esu, which was the limit of their experimental sensitivity. An expression for n_{2s} was derived by Ahkmanov et al. [25]:

$$n_{2s} = n_o(\rho dn_o/d\rho)^2/4\pi\rho v^2 \quad , \tag{2}$$

where ρ is the density and v is the radial sound velocity. At 10.6 μm, the values for NaCl are 8.3, 9.4, and 9.8 x 10^{-14} esu along the [100], [110], and [111] directions, respectively. For KCl, these values are 8.2, 11.1, and 12.6 x 10^{-14} esu. The self-focusing arising from electrostriction is incomplete until the compressive sound wave has transversed across the beam diameter.

For the electrostrictive mechanism, Kerr [26] determined two temporal regimes for the critical power P_{1s}, which for a paraboloidal temporal pulse shape, are

$$P_{1s} \approx 0.943\, P_1, \quad t > 1, \qquad \text{(steady state)} \tag{3}$$

and

$$P_{1s} \approx 0.943\, P_1/t^2, \quad t < 1, \qquad \text{(transient)} \tag{4}$$

where

$$t = \Delta t v/w_o \quad , \tag{5}$$

with w_o being the spot size at the entrance of the medium for a collimated or gently focused beam. For the bulk tests with 1.7-ns pulses and $w_o = 0.14$ mm, the value of t was 0.66 which, from eq. (4) yielded a power of 2.9 CW for P_{1s} for both NaCl and KCl along the [100] direction. This is a factor of 1000 larger than P_{1e} (2.3 and 2.9 kW, respectively),

indicating a negligible role for electrostriction in these tests. For the surface threshold tests at the same pulsewidth, electrostriction had even less influence. It had only 1% as large an effect as the electronic mechanism for the 65-ns surface tests.

From exact solutions of the nonlinear wave equation, Dawes and Marburger [27,28] suggested the use of another critical power, P_2, which gives an axial singularity at infinity for an initially plane wave. P_2 is 0.72 times larger than P_1, and for NaCl and KCl P_{2c} becomes 86 and 107 MW, respectively. To calculate the increase of the axial intensity due to self-focusing, we used formulas derived by Dawes and Marburger

$$\frac{I(z)}{I(0)} \approx [(1 - z/R)^2 + 4(1 - P/P_c)z^2/k^2w_0^4]^{-1} \quad \text{for } P < 0.25\,P_c, \tag{6}$$

and

$$\frac{I(z)}{I(0)} \approx [1 - z(1/z_f + 1/R)]^{-n/2} \quad \text{for } P < 1.5\,P_c, \tag{7}$$

where z is the path length within the medium, R is the focal length of the incident phase front within the front surface of the medium ($R = -w_0(dw/dz)_0^{-1}$, $R = 0$ for a converging beam), w_0 is the spot-size radius ($1/e^2$ level), z_f is the self focusing length and n is a numerically derived exponent. For laser powers intermediate to the above, the graphic solutions of Dawes and Marburger were used.

In the bulk tests of NaCl, the laser power levels did not exceed $0.6\,P_c$ at which self focusing produced a 0.5% intensification. In the exit-surface tests of NaCl, the ratio of P/P_c was 0.67, or less, using a spot size of 1.0 mm. The resultant intensification was computed to be less than 1% (2%) for the 1-cm (2-cm) thick samples. Comparable, but smaller, values were computed for KCl which has a smaller n_2.

Finally, we mention that Fradin et al. [29] and Smith et al. [24] have used a different formula for computing the intensification at the focus plane during bulk damage measurements:

$$\frac{I'(1)}{I(0)} \approx (1 - P/P_1)^{-1} \quad \text{for } P < 0.9\,P_1 \tag{8}$$

This formula predicts much greater intensification than is calculated from the above eq. (6) of Dawes and Marburger which describes their exact numerical solutions.

"Short-Pulse CO_2-Laser Damage Studies of NaCl and KCl Windows"

Newnam/Nowak/Gill

Figures

Figure 1. Oscillograms of CO_2 laser pulseforms.

Figure 2. Schematic of CO_2 laser damage facility and associated diagnostics.

Figure 3. Electric-field vectors of a linearly-polarized laser beam at front and rear surfaces of a transparent dielectric.

Figure 4. Exit-surface damage threshold of a single-crystal NaCl versus CO_2-laser spot-size radius.

Figure 5. Ultraviolet absorbance for several NaCl windows with the OH^- ion band at 187 nm indicated. See table 1 for sample thicknesses.

Figure 6. KCl absorption at 10.6 μm versus thickness of polished surface removed. After Turk et al. [14]

Figure 7. Bulk electric-field breakdown thresholds at 10.6 μm versus atomic density/$(n^2 - 1)$ for alkali halide crystals relative to NaCl (@1.95 MV/cm). Data from Fradin et al. [16].

Figure 8. Exit-surface damage threshold versus CO_2 laser pulsewidth for NaCl and KCl.

1.7-NS PULSE

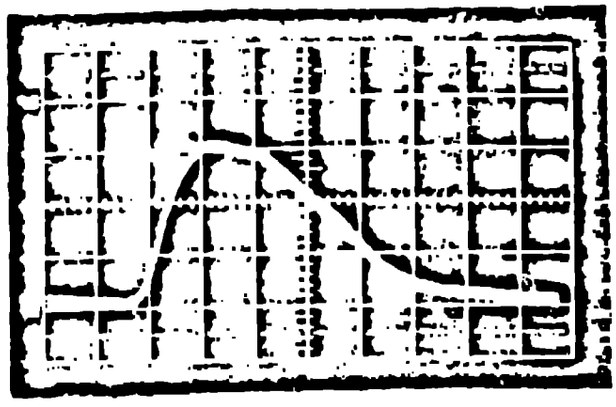

0.5 NS PER DIVISION

65-NS PULSE

20 NS PER DIVISION

Figure 1. Oscillogram of CO_2 laser pulse forms.

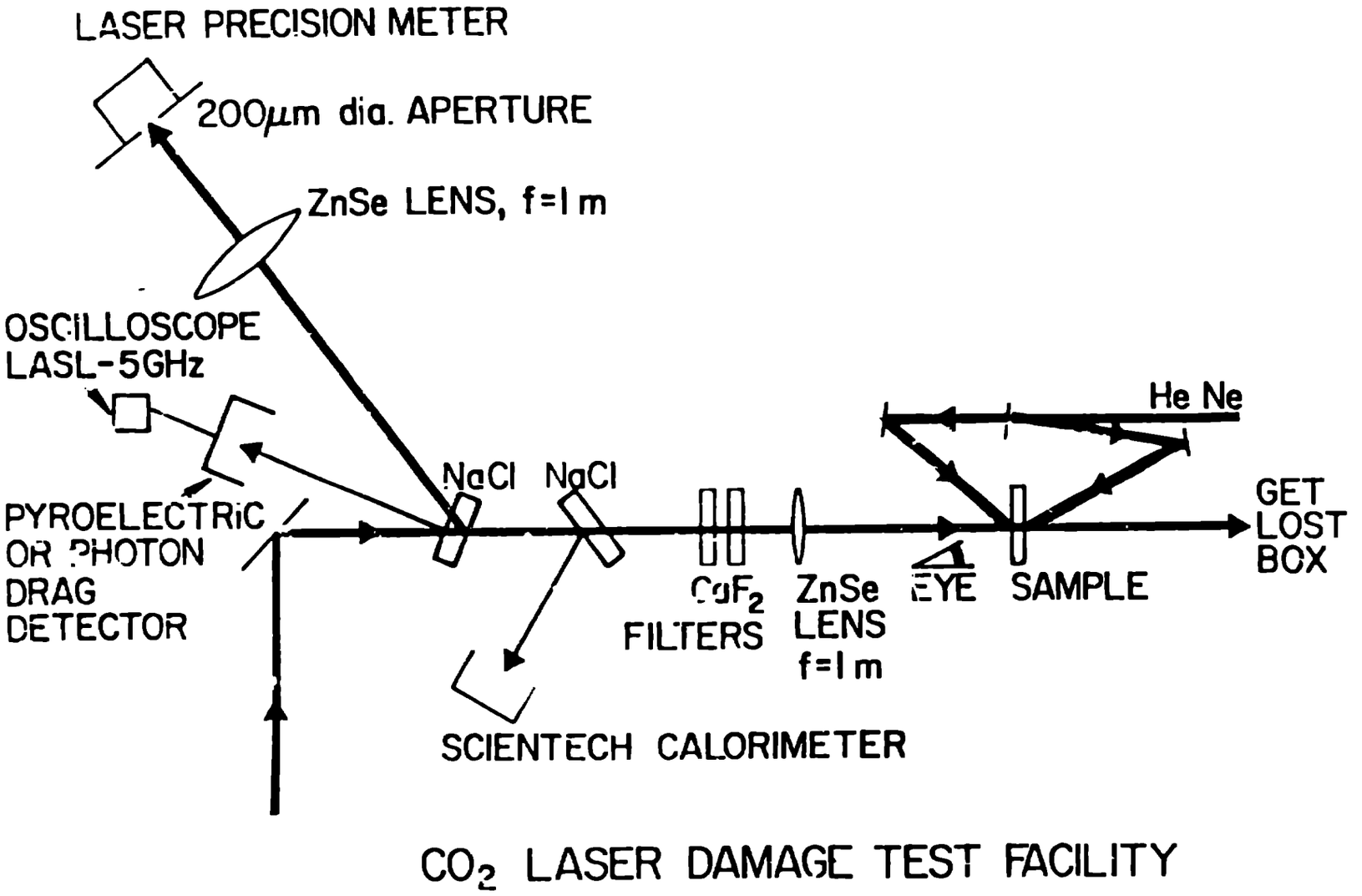

Figure 1. Schematic of CO_2 laser damage facility and associated diagnostics.

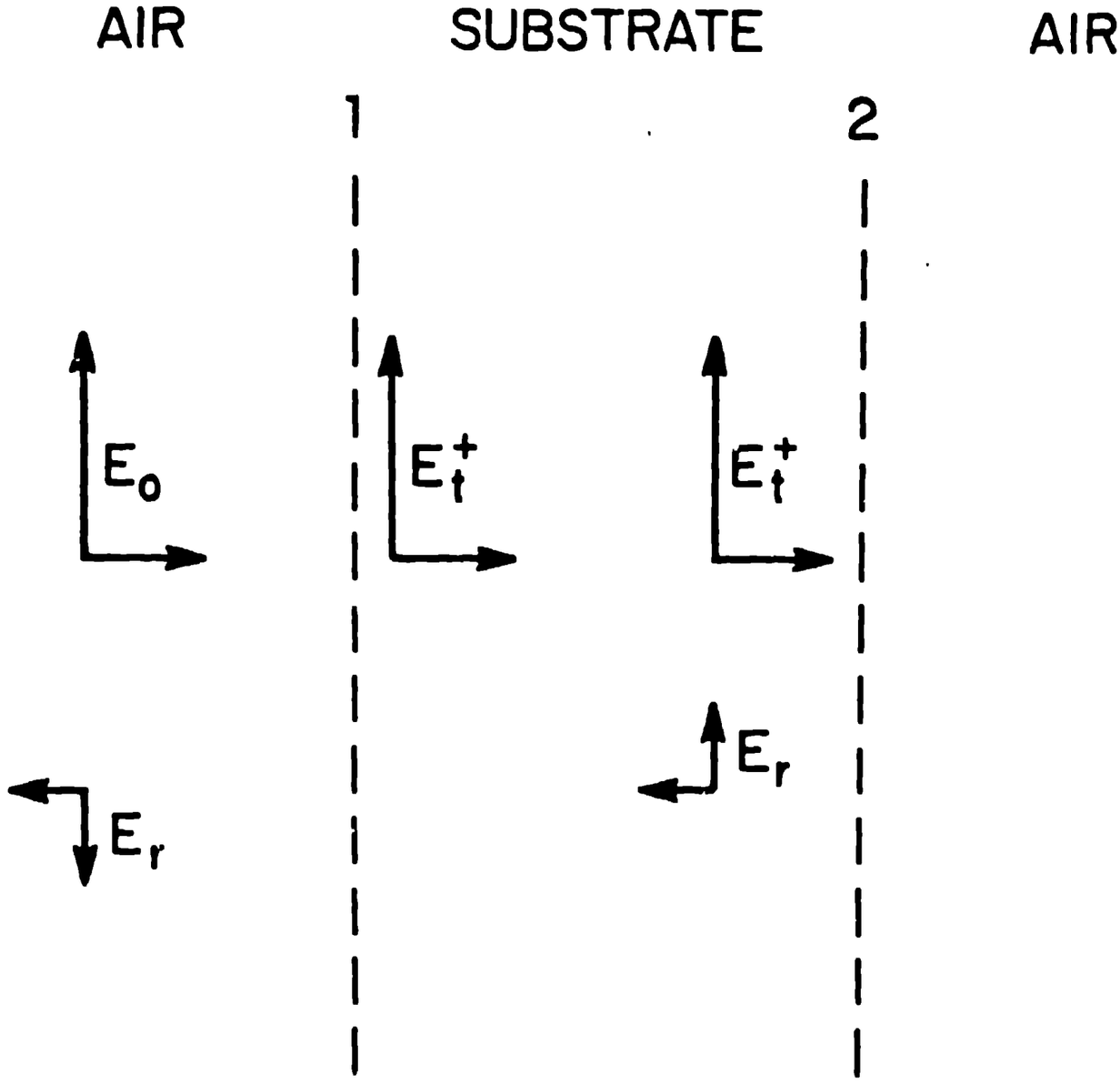

$$\frac{E\,(REAR)}{E\,(FRONT)} = \frac{2n}{|(n+1)+(n-1)\exp 2ikd|}$$

Figure 1. Electric field vectors of a linearly polarized laser beam at front and rear surfaces of a transparent dielectric.

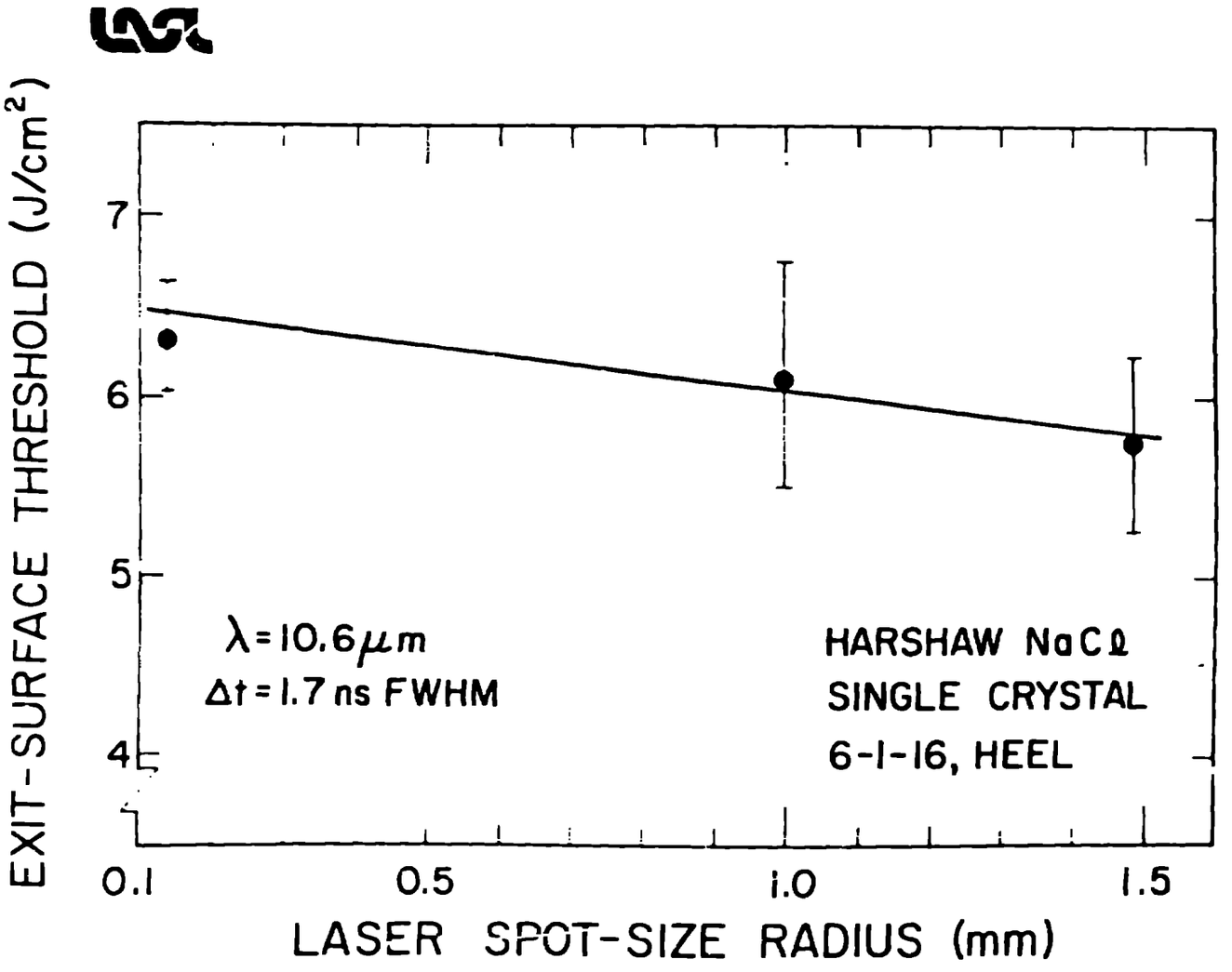

Figure 4. Exit-surface damage threshold of single-crystal NaCl versus CO_2-laser spot-size radius.

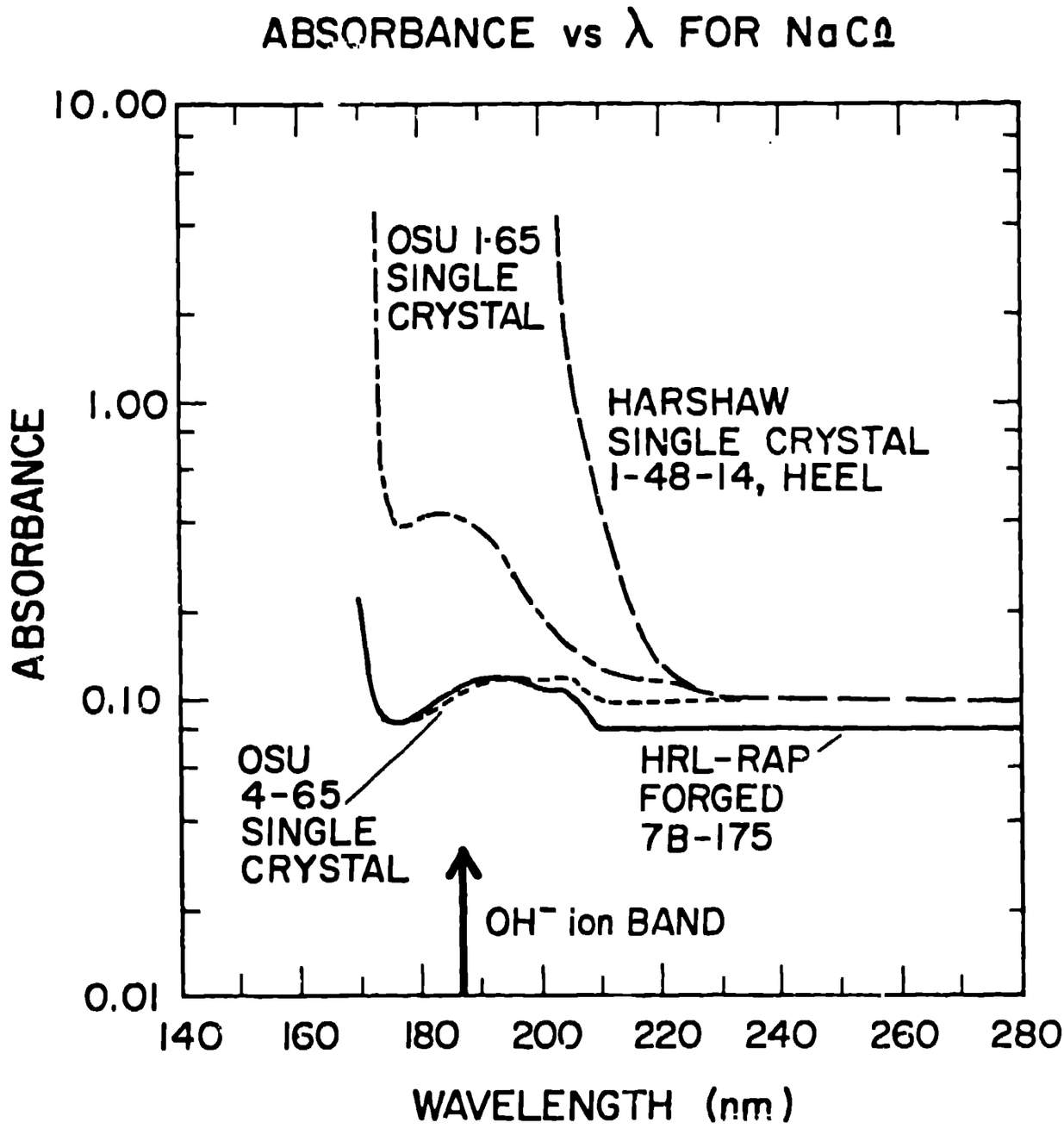

Figure 5. Ultraviolet absorbance for several NaCl windows with the OH ion band at 187 nm indicated. See table 1 for sample thicknesses.

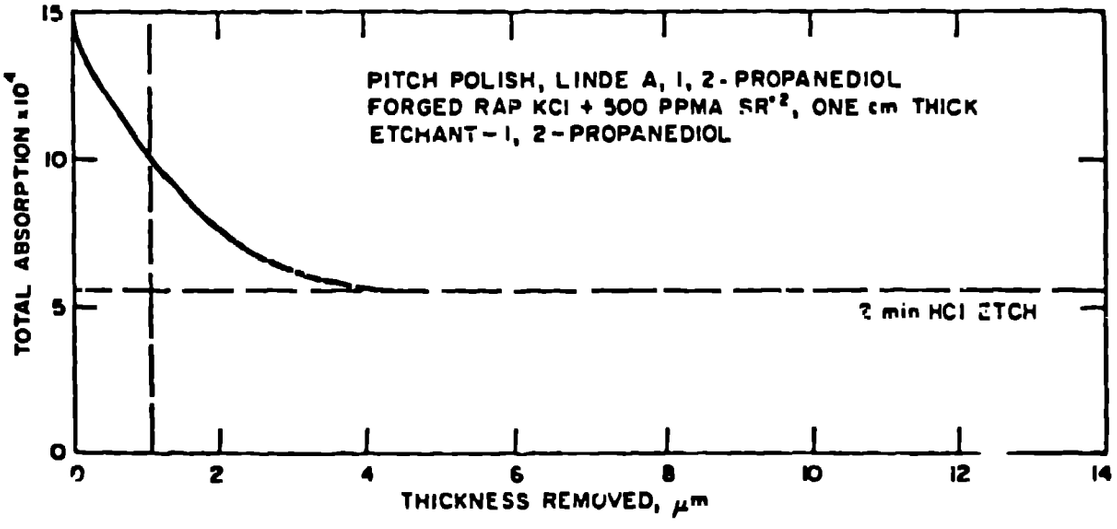

Figure 6. KCl absorption at 10.6 μm versus thickness of polished surface removed. After Turk et al. (14).

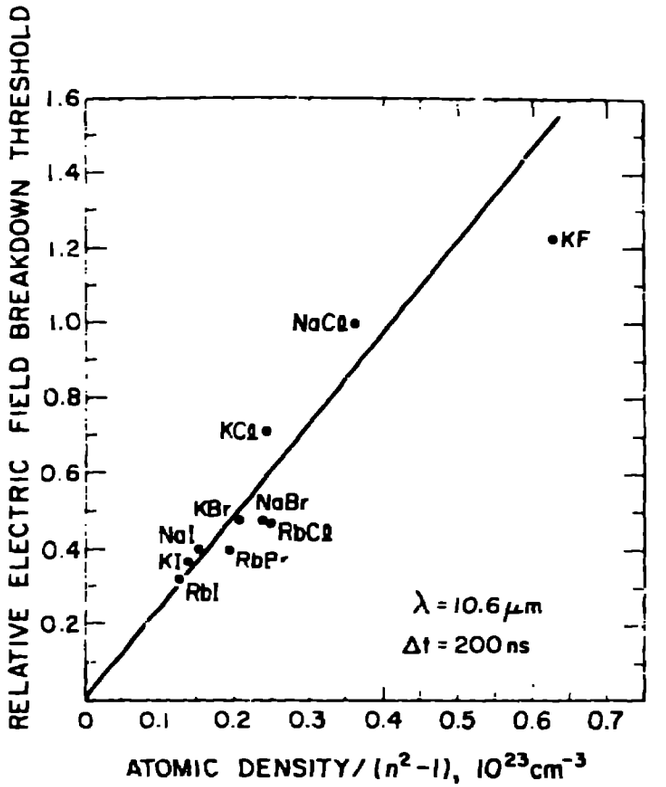

Figure 7. Bulk electric-field breakdown thresholds at 10.6 μm versus atomic density/$(n^2 - 1)$ for alkali halide crystals relative to NaCl (~1.95 MV/cm). Data from Fradin et al. (16).

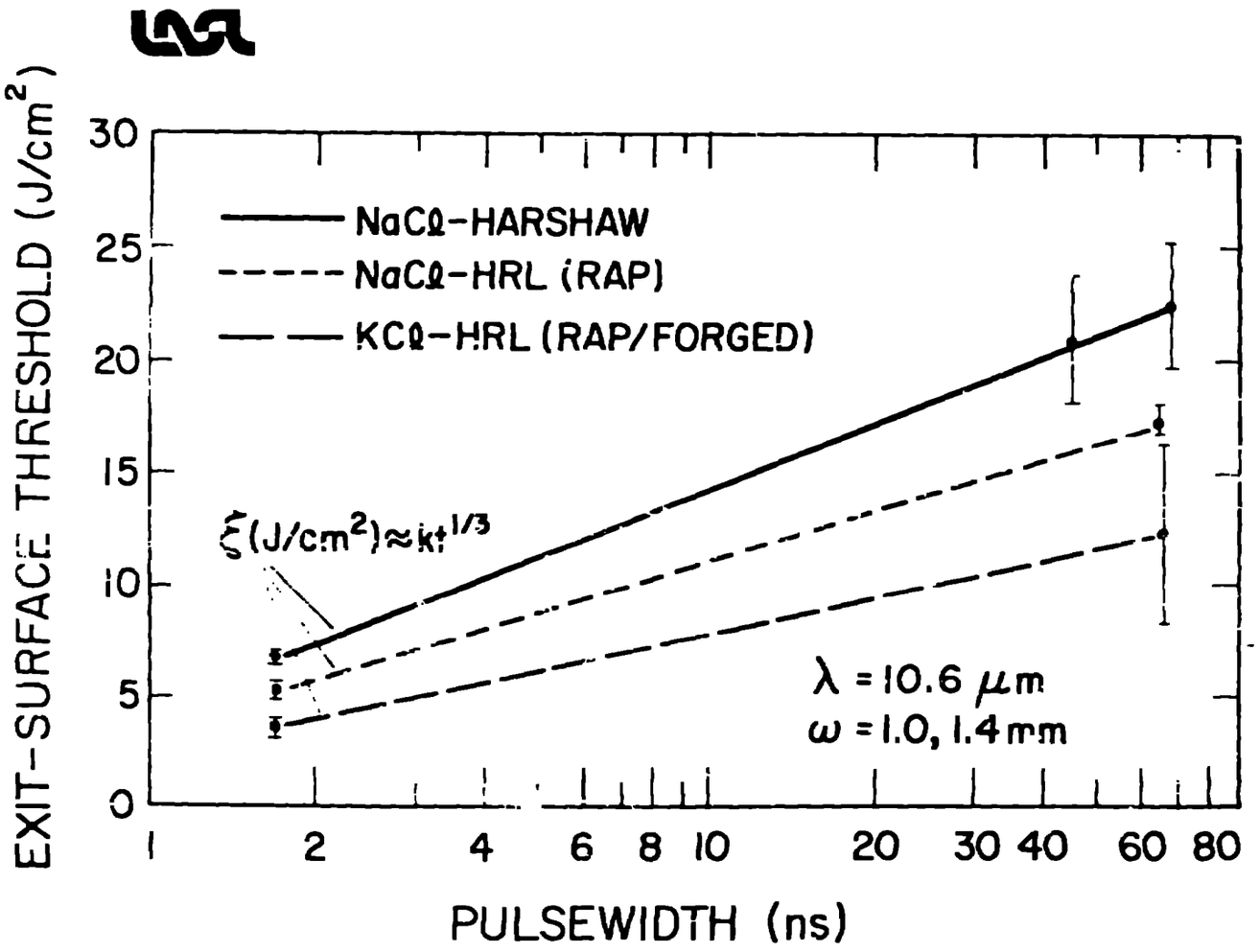

Figure 5. Exit-surface damage threshold versus CO_2 laser pulsewidth for NaCl and KCl.